Korean J. Chem. Eng., **26**(2), 468-474 (2009)

Effects of mass transfer on simulated moving bed process

Kwangnam Lee†

Department of Chemical Engineering and Research Center of Chemical Technology, Hankyong National University, 167 Jungang-ro, Anseong-si, Gyeonggi-do 456-749, Korea
(*Received 28 April 2008 • accepted 25 September 2008*)

Abstract−The objective of this work is to present the optimization of SMB operating conditions under the fixed performance of high purity (over 99%), which takes mass transfer effect into account. The parameters for the numerical calculation were used by our previous work [1,2] of binary separation of aqueous mixture of glucose and fructose. The equilibrium isotherm was linear and the mass transfer was described by LDF approximation. The single parameter of Stanton number was used for the mass transfer effect. The result of our work was compared with that of the triangle theory [3]. For the sake of this procedure, an analytical solution for a TMB mode was suggested and compared with the simulated result of SMB mode. The advantage of the TMB model with the mass transfer effect was the rapid determination of the flow conditions of each zone for the required purity of extract and raffinate.

Key words: SMB (Simulated Moving Bed), TMB (True Moving Bed), Triangle Theory, Mass Transfer Effects, Stanton Number, Numerical Simulation

INTRODUCTION

Continuous chromatography in SMB was developed to eliminate drawbacks of batch chromatography, namely dilution of species and low adsorbent utilization. In this process, an effective countercurrent flow of the adsorbent could be achieved by moving the feed and draw-off points at intervals through a fixed adsorbent bed as shown in Fig. 1(a). The liquid stream's inlet and outlet points divide the unit in four zones, each of which performs a different function. The function of Zone I is the regeneration of the adsorbent. Zone II prevents less strong adsorbed component from reaching the extract port. Zone III is to prevent the contamination of raffinate by strong adsorbed component, and the role of Zone IV is the regeneration of the desorbent.

The SMB technology has found wide applications in the areas of sugar separation, biotechnology and fine chemistry. More recent applications are related to chiral technology. The separation of enantiomers by conventional techniques is difficult because separation factors are low. Particularly, SMB technology is appropriate, provided chromatographic phases for enantiomer separation are available [4,5].

The operation of SMB chromatography is usually designed with the objective of maximizing product purity. As far as a complete separation of components is concerned, useful design methods are available that allow for a direct prediction of necessary operating conditions. The 'triangle theory' [3,6] considers only the influence of the adsorption isotherms and provides explicit expressions for optimum operating parameters. It also specifies a range of adjustable operating parameters leading to pure products. This design method has been elaborated for most of the relevant types of adsorption isotherms [7-12]. The triangle theory is based on the local equilibrium model. The equilibrium model is not able to link the product purities with the zone flow rates, zone length and mass transfer parameters, so the resulting design can serve only as an initial guess for the SMB optimization. The optimal operating conditions can be obtained by using a complete model that includes mass transfer effects. The 'standing wave analysis' [13,14] accounts for both adsorption equilibria as well as dispersive effects and requires some reconciliation using numerical models or experiments. The concept of 'separation volume' [15-18] was applied to linear and non-linear systems with mass transfer resistance and basically consists of a numerical parametric study to determine the influence of each regeneration zone on the feasibility range of the remaining parameters.

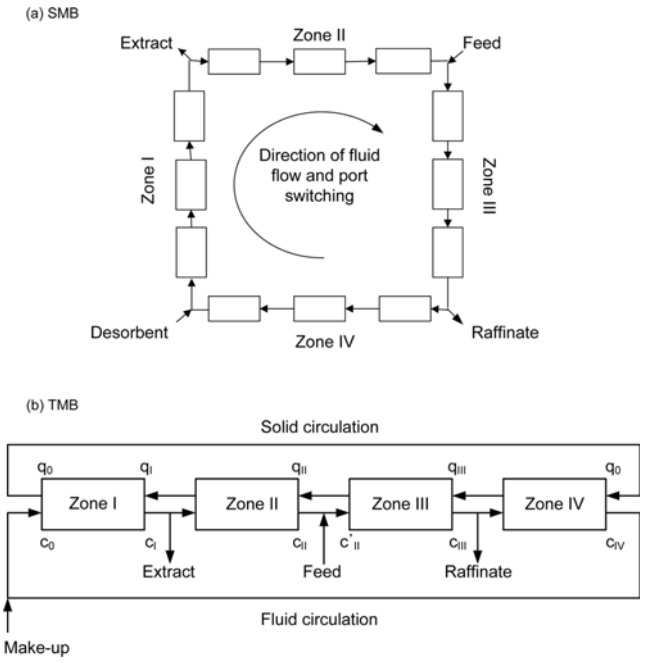

Fig. 1. Schematic diagram of (a) SMB and (b) equivalent TMB.

†To whom correspondence should be addressed.
E-mail: knlee@hknu.ac.kr

The objective of this work is (1) to develop an analytical solution for a linear SMB with mass transfer effect based on equivalence with TMB, (2) to apply this solution for the flow conditions of each zone under the fixed performance of high purity (over 99%), (3) to select these results for the performance of SMB operation, and (4) to compare it with that from the complex SMB model.

MATHEMATICAL MODEL

The performance of an SMB unit can be assessed essentially by using either one of two modeling strategies. One is an equivalent TMB unit, in which both the solid and liquid phases move in opposite directions. The other is a real SMB unit, in which the solid phase is fixed with periodic port switching.

1. TMB Model

The true moving bed is shown in Fig. 1(b). Assuming a linear driving force approximation and a linear isotherm, the basic differential equation describing the concentration profile under steady state is:

$$D_L\frac{\partial^2 c}{\partial z^2}-\upsilon\frac{\partial c}{\partial z}-\left(\frac{1-\varepsilon}{\varepsilon}\right)k(Kc-q)=0 \tag{1}$$

The adsorbed and fluid phase concentrations at the column outlet are related by an overall mass balance:

$$(q_L-q_0)(1-\varepsilon)u=\varepsilon v(c_L-c_0) \tag{2}$$

While the boundary conditions are :

$$\text{at } z=0,\ c=c_0$$

$$\text{at } z=L,\ \frac{dc}{dz}=0 \tag{3}$$

Then the expression of concentration profile is:

$$\frac{\dfrac{c}{c_0}-\dfrac{1-\dfrac{\gamma q_0}{Kc_0}}{1-\gamma}}{\dfrac{\gamma}{1-\gamma}\left(\dfrac{q_0}{Kc_0}-1\right)}=\frac{\lambda_- e^{\lambda_+\lambda_+ x}-\lambda_+ e^{\lambda_+\lambda_- x}}{\lambda_- e^{\lambda_-}-\lambda_+ e^{\lambda_+}} \tag{4}$$

Where $\gamma(=(1-\varepsilon)Ku/\varepsilon v)$ is the ratio of the downward flow in the adsorbed phase to the upward flow in the fluid phase and

$$\lambda_\pm=\frac{1}{2}[(Pe+St)\pm\sqrt{(Pe+St)^2-4PeSt(1-\gamma)}] \tag{5}$$

2. SMB Model

In the SMB process (Fig. 1(a)), each adsorption column can be considered to be a fixed bed except at the moment of moving each inlet and outlet point. The mass balance equations with the same boundary condition of Eq. (3) for each component and column can be given:

$$\frac{\partial c}{\partial t}=D_L\frac{\partial^2 c}{\partial z^2}-\upsilon_i\frac{\partial c}{\partial z}-\frac{1-\varepsilon}{\varepsilon}k_i(Kc-q) \tag{6}$$

$$\frac{\partial q}{\partial t}=k_i(Kc-q) \tag{7}$$

where the subscript i refers to the column number (1 to 12).

When feed enters column 7, the following conditions are written for the inlet points.

At the desorbent inlet point:

$$v_1c_{1,0}=v_{12}c_{12,1} \tag{8}$$

At the feed inlet point:

$$v_7c_{7,0}=v_6c_{6,1}+v_Fc_F \tag{9}$$

At the inlet points of other columns:

$$c_{i,0}=c_{i-1,1}\ (i=2,\ldots,6,8,\ldots,12) \tag{10}$$

where the first subscript is the column number and the second subscript denotes the inlet (0) and outlet (1) of the liquid stream in each column. Under the assumption that the components do not interact in the linear isotherm, the numerical solution of each fixed bed was performed through the orthogonal collocation method [19,20], which reduces the original partial differential equations to a set of ordinary ones. These differential equations were integrated through a fourth order Runge-Kutta method, and the selection of 10 collocation points at each fixed bed gave sufficient precision to calculate the theoretical profiles under run conditions of this work. When the columns were advanced at the end of a switch interval, concentration profiles corresponding to collocation points of each column were shifted by one column in the opposite direction of fluid flow according to column movement. With this procedure, the pseudo-equilibrium concentration profile can be calculated [1,2].

RESULTS AND DISCUSSION

The analytical solution of linear SMB with mass transfer effect was tested for the separation of glucose and fructose. In our previous works [1,2], the concentration profile of glucose and fructose was tested with two models: an axially dispersed flow model with constant mass transfer, and a plug flow model with velocity dependent mass transfer coefficient. Through the analysis of the method of moment [21], the performance of the two models was known to be the same, and parameters of both models are presented in Table 1. Because of simplicity, the second model was adopted here to simu-

Table 1. Parameters for axially dispersed plug flow model and plug flow model

	Axially dispersed plug flow model with constant mass transfer resistance		Plug flow model with velocity dependent mass transfer resistance	
	Glucose	Fructose	Glucose	Fructose
Equilibrium constant	0.124	0.310	0.124	0.310
Axial dispersion coefficient	0.057v	0.077v	-	-
Effective overall mass transfer coefficient	3.155	2.941	3.155v/(v+1.315)	2.941v/(v+1)

late the performance of the SMB process. Design parameters of SMB operation are listed in Table 2. In this way, mass transfer resistance and dispersion effects can be lumped into the Stanton number as a single parameter.

In the limit of plug flow of fluid phase (Pe$\rightarrow\infty$)

$$\lambda_+ \approx Pe,\ \lambda_- \approx St(1-\gamma) \tag{11}$$

Then the approximate expression of Eq. (4) is changed to :

$$(e^{st(1-\gamma)}-1/\gamma)c_0 - \frac{\gamma-1}{\gamma}c - \frac{(e^{st(1-\gamma)}-1)}{K}q_0 = 0 \tag{12}$$

For each section of 4 zones of the TMB system as shown in Fig. 1(b), we have one equation of type (12) and one equation of type (2) relating the inlet and outlet concentrations, thus giving, in all, eight equations relating the ten concentrations q_0, q_I, q_{II}, q_{III}, c_0, c_I, c_{II}, c'_{II}, c_{III} and c_{IV}. Two additional equations are obtained from the mass balance over the feed point and recirculating stream:

$$Fc_F+(D-E)c_{II}=(D-E+F)c'_{II} \tag{13}$$

$$(D-E+F-R)c_{IV}=Dc_0 \tag{14}$$

With the flow rates, the Stanton number and equilibrium constant all defined, the solutions to this set of equations give the steady state concentration profile. Since the equations are linear, the solution is obtained in a straightforward manner.

Simulated moving bed operation is achieved by advancing the desorbent, extract, feed and raffinate points at fixed time intervals by one column in the direction of fluid flow as shown in Fig. 1(a). In the operation principle of the SMB unit, the solid phase of the column is count-currently moved to the direction of mobile phase flow at a fixed rate; that is, the slow-moving component can be made to travel with the solid phase and the fast-moving component with the mobile phase. The essential requirement to achieve a good separation in such a process is that the flow rates in four sections must be adjusted in such a way as to achieve a net flow of the more strongly adsorbed species toward the extract point, and a net flow of the less strongly adsorbed species toward the raffinate point. Since fructose is the slow-moving component and glucose is the fast-moving component in the cation exchanged resin [1], the flow ratio of the downward flow in the adsorbed phase to the upward flow in the mobile phase ($\gamma=(1-\varepsilon)Ku/\varepsilon v$) can be specified for a linear system.

Zone I	$\gamma_G<1.0$	$\gamma_F<1.0$
Zone II	$\gamma_G<1.0$	$\gamma_F>1.0$
Zone III	$\gamma_G<1.0$	$\gamma_F>1.0$
Zone IV	$\gamma_G>1.0$	$\gamma_F>1.0$

(15)

Table 2. SMB design parameters

Temperature	40 °C
Column configuration	3-3-3-3
Column diameter	1 cm
Column length	30 cm
Adsorbent	Dowex 50W-X12 resin of Ca^{++} form
Void fraction	0.372
Desorbent	Deionized water
Feed concentration	10 g/*l*

These flow ratios can be conveniently converted to m-planes ($m_i=\varepsilon v_i/(1-\varepsilon)u_i$) according to triangle theory [3].

$$m_1>K_F \tag{16}$$

$$K_G<m_2<m_3<K_F \tag{17}$$

$$m_4<K_G \tag{18}$$

These inequalities define the complete separation region of TMB operation for the linear equilibrium binary separation in the absence of dispersion and mass transfer effect as shown in Fig. 2.

In the restricted condition of high purity (over 99%), the separation region could be obtained by scanning the triangle region of the equilibrium model. In Fig. 3, it can be observed that, for a fixed value

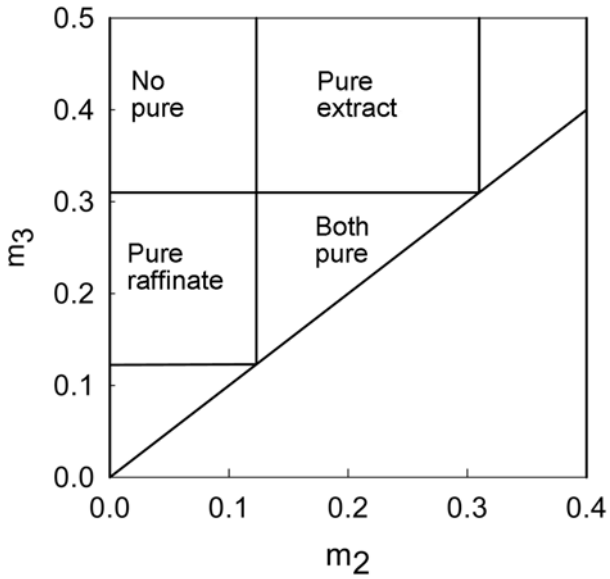

Fig. 2. Region of complete separation region for glucose (K_G=0.124) and fructose (K_F=0.310) mixture according to equilibrium model.

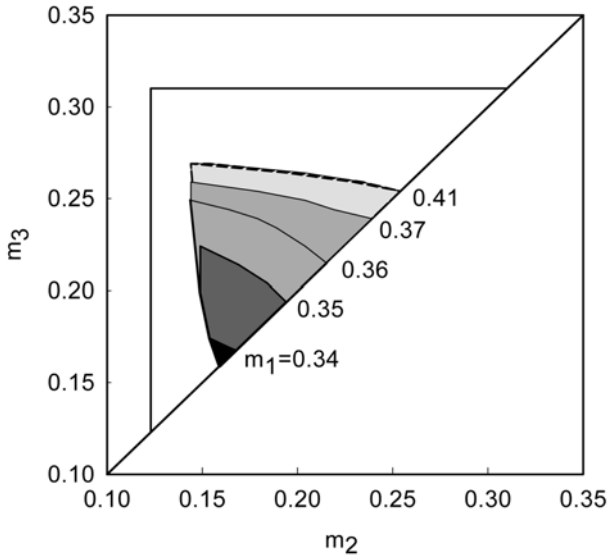

Fig. 3. Region of complete separation in terms of m_1 under m_4= 0.08.

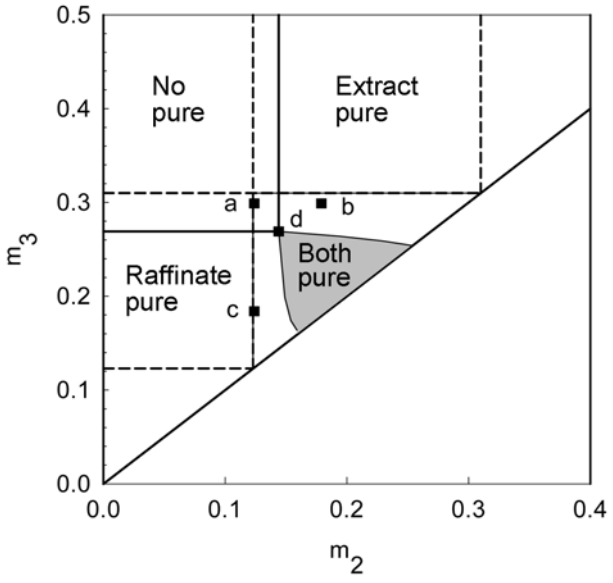

Fig. 4. Representation of Run conditions in $m_2 \times m_3$ plane with m_1= 0.36 and m_4=0.08.

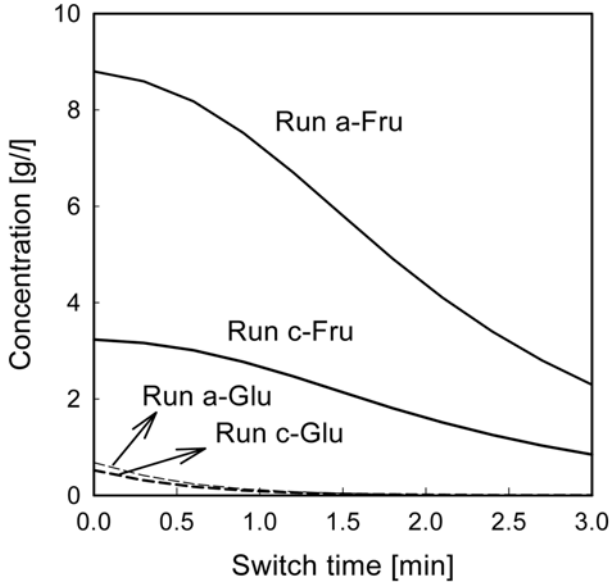

Fig. 5. Concentration profiles of Run a and c in the extract port predicted by SMB model.

of m_4 which meets Eq. (18), the separation region increases by increasing m_1 up to 0.41; further increase of m_1 does not influence the size of separation region. To confirm the calculation results of the TMB model, run conditions of a-d in Fig. 4 and Table 3 were tested by the SMB model. As each column contains the desorbent phase in the void volume, such amount has to be compensated for the desorbent rate to get the actual desorbent rate in the SMB unit.

$$D' = D + A\varepsilon u \quad (19)$$

Although runs a-c were satisfied by Eq. (17) of equilibrium model, complete separation was not obtained due to the dispersion and mass transfer effects. The calculated results of the SMB model are shown in Figs. 5 and 6 and also Table 4. When SMB is operated with improper flow rates, the contamination of extract always appears in early time of a switch and raffinate in later as shown in Figs. 5 and 6.

When the size of the separation region increases, the vertex moves from lower to higher value of (m_2, m_3), which means a higher feed flow rate and high productivity. Further increasing m_1 than 0.41 in-

Table 3. SMB operating conditions

Run	Switch time [min]	Flow rate of each zone [ml/min] Q_1, Q_2,Q_3, Q_4	m values of zone II and III m_2, m_3	St values of zone II and III (St_G, St_F)
a	3	2.02, 0.61, 1.47, 0.39	0.124, 0.299	(17.44, 17.91) (22.53, 22.09)
b	3	2.02, 0.88, 1.47, 0.39	0.179, 0.299	(19.79, 19.88) (22.53, 22.09)
c	3	2.02, 0.61, 0.91, 0.39	0.124, 0.184	(17.44, 17.91) (19.95, 20.02)
d	3	2.02, 0.71, 1.33, 0.39	0.144, 0.269	(18.42, 18.75) (21.63, 21.38)
e	4	1.52, 0.51, 1.01, 0.30	0.139, 0.274	(21.67, 22.50) (27.45, 27.39)
f	5	1.21, 0.40, 0.84, 0.24	0.134, 0.284	(24.14, 25.39) (32.48, 32.72)
g	6	1.01, 0.33, 0.71, 0.20	0.134, 0.289	(26.26, 28.09) (36.90, 37.53)

*for all conditions, m_1=0.41 and m_4=0.08

Table 4. Purities of extract and raffinate

Run	TMB model		SMB model			
	Extract purity	Raffinate purity	Extract purity	Raffinate purity	Extract recovery	Raffinate recovery
a	96.62	95.54	98.29	96.48	89.07	119.89
b	99.96	94.10	99.98	95.55	85.34	125.02
c	91.69	99.94	96.51	100.00	94.13	144.91
d	99.18	99.02	99.64	99.26	92.15	126.94
e	99.22	99.42	99.81	99.50	92.11	126.07
f	99.06	99.25	99.71	99.62	92.24	126.26
g	99.25	99.19	99.88	99.53	91.54	126.57

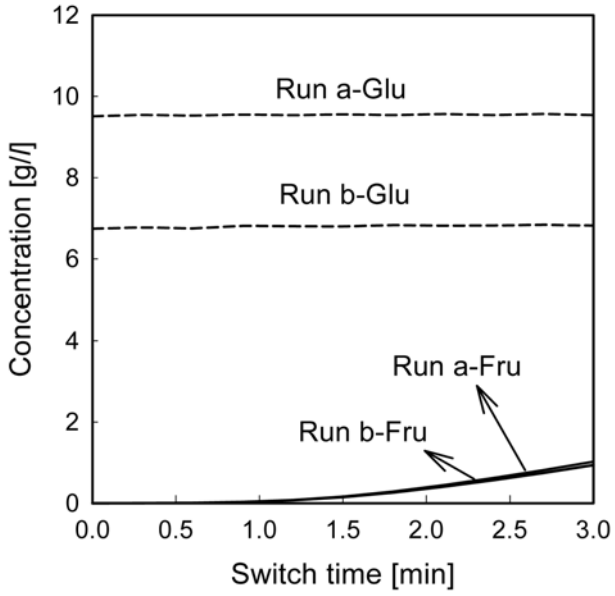

Fig. 6. Concentration profiles of Run a and b in the raffinate port predicted by SMB model.

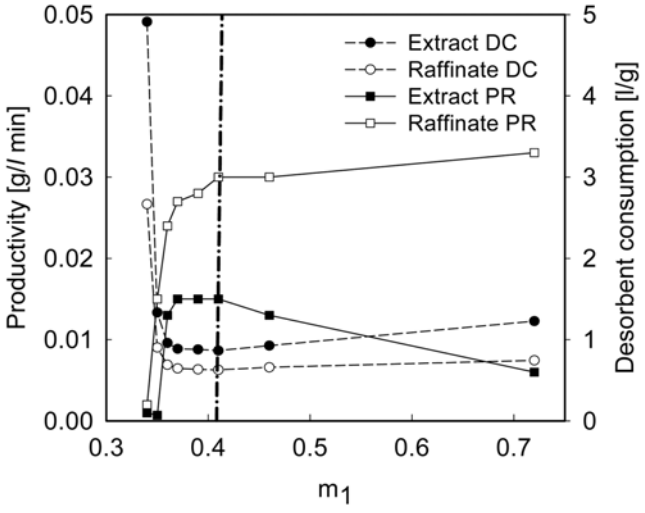

Fig. 7. Influence of m_1 on SMB performance for switch interval, 3 min and m_4=0.08.

Table 5. Performance parameters

SMB performance	Extract	Raffinate
Purity [%]	$PU_{EX}=100\times\frac{\bar{c}_{F,EX}}{\bar{c}_{F,EX}+\bar{c}_{G,EX}}$	$PU_{RF}=100\times\frac{\bar{c}_{G,RF}}{\bar{c}_{G,RF}+\bar{c}_{F,RF}}$
Productivity [g/*l* min]	$PR_{EX}=\frac{\bar{c}_{F,EX}E}{V_{ads}}$	$PR_{RF}=\frac{\bar{c}_{G,RF}R}{V_{ads}}$
Solvent consumption [*l*/g]	$SC_{EX}=\frac{D}{\bar{c}_{F,EX}E}$	$SC_{RF}=\frac{D}{\bar{c}_{G,RF}R}$
Recovery [%]	$RC_{EX}=100\times\frac{\bar{c}_{F,EX}E}{\bar{c}_{F,FD}F}$	$RC_{RF}=100\times\frac{\bar{c}_{G,RF}R}{\bar{c}_{G,FD}F}$

fluences neither the position nor the size of the separation region, and more desorbent is used to dilute the product. This effect is shown in Fig. 7, and the performance parameters used in SMB process are summarized in Table 5. When the separation region does not increase more, a further increase in m_1 does not affect the feed flow rate and SMB productivity, since feed flow rate is determined by m_3-m_2. When m_1 increases over 0.41 as in Fig. 7, the productivity of extract eventually decreases and desorbent consumptions in the extract and raffinate increase. With the switch interval of 3 min, the m_1 value of 0.41 seems to be the proper operating condition. This value was used for the test of m_4 effect.

The separation regions were calculated for different values of m_4 by fixing the value of m_1. When the value of m_1 was fixed to 0.41, the shape of the separation region was no more changed. Fig. 8 shows the performance of the SMB process with various m_4 values. Near the equilibrium value (K_G=0.124), separation of high purity is not

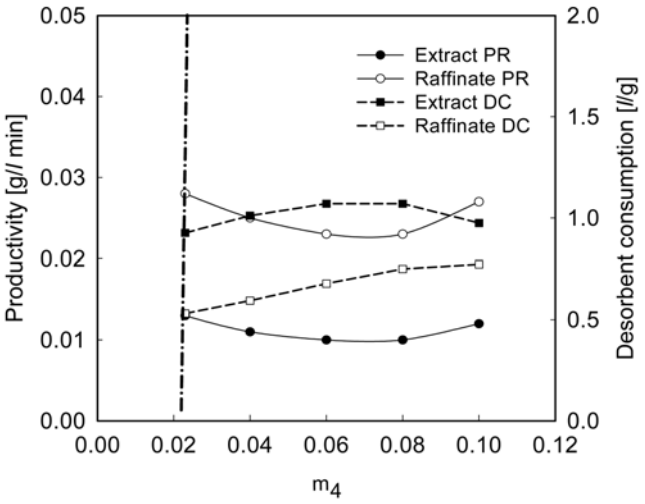

Fig. 8. Influence of m_4 on SMB performance for switch interval, 3 min and m_1=0.41.

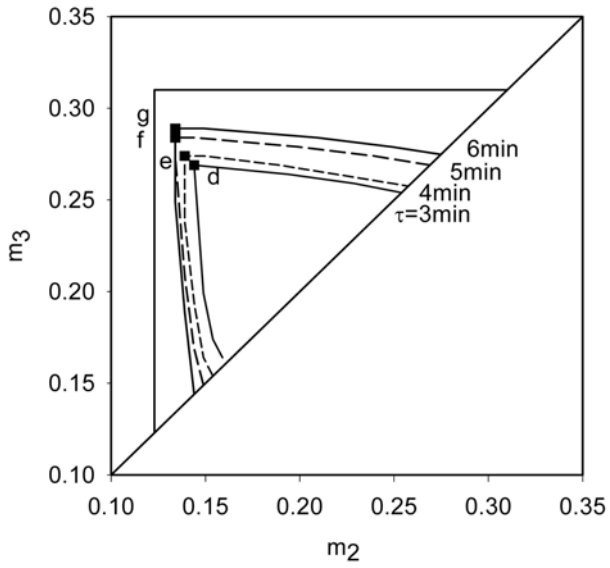

Fig. 9. Region of complete separation in terms of switch time under m_1=0.41 and m_4=0.08.

possible. As m_4 decreases, the productivity increases and desorbent consumption decreases. For a fixed switch time of 3 min, it is convenient to use a higher value of m_1 and lower value of m_4 than those imposed by triangle theory. But the use of high m_1 and low m_4 will increase the desorbent required and thus the dilution of each product. Therefore, the optimal operating conditions for m_1 and m_4 will be between these two conditions.

The effect of switch time, which is one of the operating parameters, was also tested. As the switch time increases, the separation zone increases as shown in Fig. 9. Stanton number increases according to increasing switch time. This effect is well explained in Table 3. When the Stanton number is infinite, the separation zone is equal to the triangle of the equilibrium model. Thus as Stanton number increases, the separation zone also increases as shown in Fig. 10. In this figure, the separation zone was calculated under the fixed m_1 and m_4 condition. The SMB performance of runs d-g in Fig. 9 is shown in Fig. 11. All conditions were selected from the vertex of each separation zone. As the vertex moved to a higher value of (m_2, m_3) according to the switch time increasing, the productivity would be estimated to increase according to feed increasing. But the productivity and desorbent consumption were closely related to the flow rates of each inlet and outlet port. Although the desorbent consumption increases, a short switch interval is proper to get high productivity.

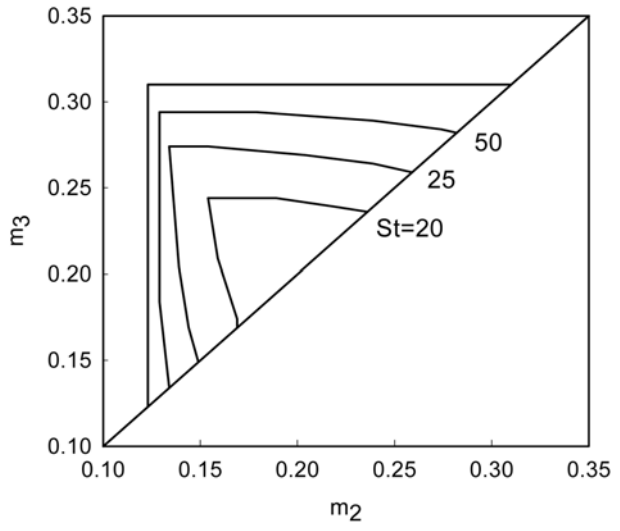

Fig. 10. Region of complete separation in terms of Stanton number under m_1=0.41 and m_4=0.08.

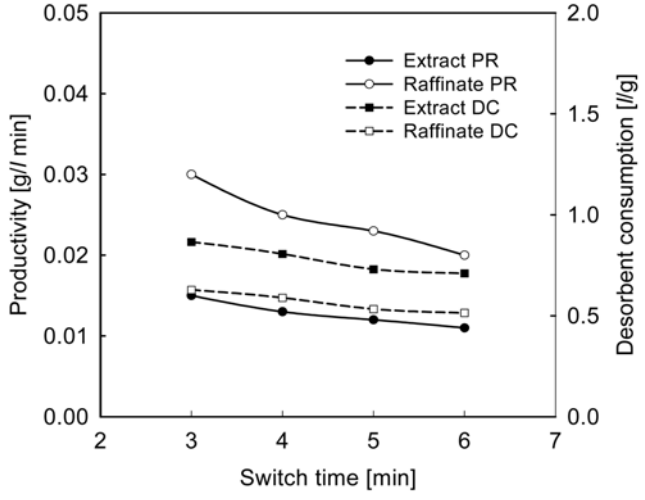

Fig. 11. Productivity and desorbent consumption for Run d-g.

CONCLUSION

The solution of the steady state equivalent TMB model for a linear SMB was used to predict the performance of SMB operation under the restricted conditions of high purity (over 99%). Dispersion and mass transfer effects were lumped into the Stanton number as a single parameter. This solution was a set of linear algebraic equations and provided a rapid determination of the flow rates of each zone for the complete separation and performance of SMB operation. These results were confirmed by the complex transient SMB model and two calculated results were identical.

NOMENCLATURE

A : cross sectional area of column [cm^2]
c : fluid phase concentration [g/*l*]
$\bar{c}$: average concentration at extract and raffinate port [g/*l*]
c_F : feed concentration [g/*l*]
D : desorbent flow rate [ml/min]
D′ : actual desorbent flow rate [ml/min]
E : extract flow rate [ml/min]
F : feed flow rate [ml/min]
K : adsorption equilibrium constant [=q*/c]
k : effective overall mass transfer coefficient [min^{-1}]
L : length of adsorbed bed [cm]
LDF : linear driving force
m_i : ratio of fluid flow to solid flow of each zone of TMB
Pe : peclet number, vL/D_L [-]
q : adsorbed phase concentration [g/*l*]
Q_i : flow rate of each zone [ml/min]
R : raffinate flow rate [ml/min]
S : hypothetical adsorbent recirculation rate in equivalent counter current system [ml/min]
SMB : simulated moving bed
St : stanton number, kL/u [-]
t : time [min]
TMB : true moving bed
u : hypothetical solid velocity (=L/τ) [cm/min]
v : interstitial fluid phase velocity [cm/min]
v_f : feed velocity [cm/min]

Greek Letters

γ : dimensionless parameter [=(1−ε)Ku/εv]
ε : void fraction of packed bed
τ : switch time [min]

Subscript

F : Fructose
G : Glucose
DE : Desorbent

EX : Extract
FD : Feed
RF : Raffinate

REFERENCES

1. K. N. Lee and W. K. Lee, *Sep. Sci. Tech.*, **27**(3), 295 (1992).
2. K. N. Lee., *Korean J. Chem. Eng*., **20**, 532 (2003).
3. M. Mazzotti, G. Storti and M. Morbidelli, *J. Chromatogr. A*, **769**, 3 (1997).
4. L. S. Pais, J. M. Loureiro and A. E. Rodrigues, *J. Chromatogr. A*, **769**, 25 (1997).
5. T. H. Yoon, E. Lee, J. M. Kim, W. S. Kim and I. H. Kim, *Korean J. Chem. Eng.*, **25**, 285 (2008).
6. G. Storti, R. Baciocchi, M. Mazzotti and M Morbidelli, *Ind. Eng. Chem. Res.*, **34**, 288 (1995).
7. G. Storti, M. Mazzotti, M. Morbidelli and S. Carra, *AIChE J.*, **39**, 471 (1993).
8. M. Mazzotti, G. Storti and M. Morbidelli, *AIChE J.*, **40**, 1825 (1994).
9. M. Mazzotti, G. Storti and M. Morbidelli, *AIChE J.*, **42**, 2784 (1996).
10. M. Mazzotti, G. Storti and M. Morbidelli, *AIChE J.*, **43**, 64 (1997).
11. C. Migliorini, M. Mazzotti and M. Morbidelli, *AIChE J.*, **46**, 1384 (2000).
12. M. Mazzotti , *J. Chromatogr. A*, **1126**, 311 (2006).
13. Z. Ma and N. H. L. Wang, *AIChE J.*, **43**, 2488 (1997).
14. T. Mallmann, B. D. Burris, Z. Ma and N. H. L. Wang, *AIChE J.*, **44**, 2628 (1998).
15. M. Minceva and A. E. Rodgrigues, *Comp. Chem. Eng.*, **29,** 2215 (2005).
16. D. C. S. Azevedo and A. E. Rodrigues, *AIChE J.*, **45**, 956 (1999).
17. V.Silva, M. Minceva and A. E. Rodrigues, *Ind. Eng. Chem. Res.*, **43**, 4494 (2004).
18. A. E. Rodrigues and L. S. Pais, *Sep. Sci. Technol.*, **39**, 245 (2004).
19. J. Villadsen and M. L. Michelson, *Solution of differential equation models by polynomial approximation*, Prentice Hall, Englewood Cliffs, NJ (1980).
20. B. A. Finlayson, *Nonlinear analysis in chemical engineering*, McGraw-Hill, Hew York (1980).
21. C. V. Goncalves, M. J. S. Carpes, C. R. D. Correa and C. C. Santana, *Chem. Eng. J.*, **133**, 151 (2007).